

# ARE BILINEAR QUADRILATERALS BETTER THAN LINEAR TRIANGLES?\*

E. F. D'AZEVEDO<sup>†</sup>

**Abstract.** This paper compares the theoretical effectiveness of bilinear approximation over quadrilaterals with linear approximation over triangles. Anisotropic mesh transformation is used to generate asymptotically optimally efficient meshes for piecewise linear interpolation over triangles and bilinear interpolation over quadrilaterals. For approximating a convex function, although bilinear quadrilaterals are more efficient, linear triangles are more accurate and may be preferred in finite element computations; whereas for saddle-shaped functions, quadrilaterals may offer a higher order approximation on a well-designed mesh. A surprising finding is different grid orientations may yield an order of magnitude improvement in approximation accuracy.

**Key words.** mesh generation, interpolation, quadrilateral patch, triangulation, bilinear approximation

**1. Introduction.** This paper compares the theoretical effectiveness of bilinear approximation over quadrilaterals with linear approximation over triangles. The novelty is in the use of anisotropic mesh transformation to generate asymptotically optimally efficient meshes in the comparison. Elementary analysis based on a simple quadratic data model is used. Although both linear and bilinear interpolants are  $O(h^2)$  accurate, the results suggest linear triangles are *always* more accurate than general convex bilinear quadrilaterals in approximating a convex function but bilinear approximation may offer a higher order approximation for saddle-shaped functions on a well-designed mesh. A surprising finding is different grid orientations may yield an order of magnitude “super-convergence” improvement in approximation accuracy. This work is a basic study on optimal meshes with the intention of gaining insight into the more complex meshing problems in finite element analysis.

We consider the problem of interpolating a given smooth data function with continuous piecewise linear triangles or bilinear quadrilaterals over a domain to satisfy a given error tolerance. A mesh that achieves this error tolerance with the *fewest* elements is defined to be optimally efficient. Intuitively, one would expect smaller and denser elements in regions where the function has sharp peaks or large variations. Since each convex quadrilateral can be split across either one of the diagonals into two triangles, one can imagine embedding a refined triangular mesh within the quadrilateral mesh. A practical question arises as to whether the bilinear approximation over quadrilaterals or linear approximation over triangles is more effective.

To make a fair comparison, we need to compare bilinear approximation over an “optimal” quadrilateral mesh versus linear approximation over an “optimal” triangular mesh. Provably optimal triangular meshes [2, 4] have been produced by anisotropic mesh transformation.

Anisotropic mesh transformation is emerging as an effective technique for unstructured grid generation where the vertex distribution is highly non-uniform. The central idea is to control the element shapes and sizes by specifying a symmetric met-

---

\* This work was supported by the Applied Mathematical Sciences subprogram of the Office of Energy Research, U.S. Department of Energy, under contract DE-AC05-84OR21400 with Lockheed Martin Energy Systems, Inc.; and in part by the Information Technology Research Centre, which is funded by the Province of Ontario.

<sup>†</sup>Mathematical Sciences Section, Oak Ridge National Laboratory, P. O. Box 2008, Building 6012, Oak Ridge, TN 37831-6367, email: e6d@ornl.gov.

ric tensor that measures the approximation error. The metric tensor determines the corresponding anisotropic transformation. The anisotropic mesh is then the image of a uniform mesh of optimal shape elements under the anisotropic transformation. Simpson [8] gives a survey on anisotropic meshes.

Nadler [6], D'Azevedo and Simpson [3, 4], and D'Azevedo [2] have studied *local* anisotropic transformation for the generating of optimally efficient triangular meshes. Peraire et al. [7] applied anisotropic transformation in mesh generation for dynamic remeshing in solving compressible flow problems. In these works, piecewise linear approximation of a quadratic function is used as the model for local analysis. In this paper we extend a similar analysis to bilinear approximation on quadrilateral patches.

An outline of the paper follows. In §2, we review the key ideas in [2] for generating optimally efficient triangular meshes. In §3, we consider error properties of bilinear interpolation. We consider the optimal geometry for quadrilateral patches in §4. We compare the effectiveness of quadrilaterals versus triangular meshes using the local quadratic model in §5. Numerical experiments and the results are described in §6. Finally §7 gives a brief summary.

**2. Triangular Patch.** This section is a brief review of the basic ideas in [2] for determining optimal triangle geometry. We show a linear transformation of a regular mesh of optimal-shape triangles yields an optimally efficient mesh for interpolating a quadratic function.

**2.1. Quadratic Model.** We shall consider a local analysis where we assume the data function  $f(x, y)$  in the neighborhood of  $(x_c, y_c)$  is well approximated by its quadratic Taylor expansion,

$$(2.1) \quad \begin{aligned} f(x, y) &= f(x_c + dx, y_c + dy) \\ &\approx f(x_c, y_c) + \nabla f(x_c, y_c)[dx, dy] + \frac{1}{2}[dx, dy]H[dx, dy]^t. \end{aligned}$$

Let the error formula be  $E_T(x, y) = p_\ell(x, y) - f(x, y)$ , where  $p_\ell(x, y)$  is the linear interpolant. By our assumption,  $E_T(x, y)$  is a quadratic function and level curves for  $E_T(x, y) = c$  form a family of conics with a common center at  $(x_c, y_c)$ . They form a family of ellipses if  $\det(H) > 0$ , and hyperbolas if  $\det(H) < 0$ . Note by the interpolation condition, the curve  $E_T(x, y) = 0$  passes through all vertices of the triangle. If  $\det(H) > 0$  (conic is an ellipse) then  $E_T(x, y)$  attains the local maximum at the center  $(x_c, y_c)$ ; otherwise,  $\det(H) < 0$  (conic is a hyperbola) the maximum error is attained at the midpoint of an edge. The error at a displacement from the center is given by

$$(2.2) \quad E_T(x_c + dx, y_c + dy) = E_T - \frac{1}{2}[dx, dy]H[dx, dy]^t, \quad E_T = E_T(x_c, y_c).$$

The key insight in [2] is in interpreting the Hessian matrix  $H$  in (2.2) as a symmetric metric tensor. Let the symmetric Hessian matrix be diagonalizable as

$$(2.3) \quad \begin{aligned} H &= Q^t \begin{bmatrix} \lambda_1 & 0 \\ 0 & \lambda_2 \end{bmatrix} Q = S^t \begin{bmatrix} 1 & 0 \\ 0 & \epsilon \end{bmatrix} S, \quad \text{where } \epsilon = \text{sign}(\det(H)), \\ S &= \begin{bmatrix} \sqrt{|\lambda_1|} & 0 \\ 0 & \sqrt{|\lambda_2|} \end{bmatrix} Q, \quad \text{and } Q \text{ is orthogonal, } Q^t Q = I. \end{aligned}$$

Note that transformation  $S$  is essentially a rotation to align eigenvectors along the coordinate axes then followed by a simple scaling. Under this transformation  $S$ , the

expression  $[dx, dy]H[dx, dy]^t$  reduces to  $(d\tilde{x})^2 + \epsilon(d\tilde{y})^2$ , where  $[\tilde{x}, \tilde{y}]^t = S[x, y]^t$ . The error function can be rewritten as

$$\begin{aligned}
 E_T(x_c + dx, y_c + dy) &= E_T - \frac{1}{2}[dx, dy]H[dx, dy]^t \\
 (2.4) \qquad \qquad \qquad &= E_T - \frac{1}{2}((d\tilde{x})^2 + \epsilon(d\tilde{y})^2) \\
 &= \tilde{E}_T(\tilde{x}_c + d\tilde{x}, \tilde{y}_c + d\tilde{y}),
 \end{aligned}$$

where  $\tilde{E}_T(\tilde{x}, \tilde{y})$  denotes the corresponding error function under transformation  $S$  in  $(\tilde{x}, \tilde{y})$ -space. The error expression  $\tilde{E}_T(\tilde{x}, \tilde{y})$  has no preferred direction (except for the sign), hence we shall call the  $(\tilde{x}, \tilde{y})$ -space the ‘‘isotropic’’ space.

**2.2. Optimal shape.** In the following, we shall determined the best triangle shape that minimizes the interpolation error. We can determine the ‘‘efficiency’’ of the elements by computing their ratio of Error to Area. A small ratio indicates a more efficient element, i.e. one can achieve a lower error tolerance and tile the domain with about the same number of elements.

We consider first the case  $f(x, y)$  is convex ( $\det(H) > 0$ ,  $\epsilon = 1$ ) and level curves or contours of  $\tilde{E}_T(\tilde{x}, \tilde{y})$  are concentric circles given by

$$(2.5) \qquad \tilde{E}_T(\tilde{x}_c + d\tilde{x}, \tilde{y}_c + d\tilde{y}) = E_T - \frac{1}{2}((d\tilde{x})^2 + (d\tilde{y})^2) .$$

Let  $\tilde{T}$  be the transformed image of triangle  $T$  over the isotropic space, with vertices at  $(\tilde{x}_1, \tilde{y}_1)$ ,  $(\tilde{x}_2, \tilde{y}_2)$  and  $(\tilde{x}_3, \tilde{y}_3)$ . The circum-circle of  $\tilde{T}$  corresponds to the level curve of value zero. Hence the radius of this circum-circle is  $\sqrt{2|E_T|}$  and relates directly to the maximum error attainable (at the center). If this center is exterior to triangle  $T$ , the maximum error is attained at the mid-point of the longest edge (of length  $L$ ) with value  $L^2/8$ . We can easily see that an equilateral triangle covers the most area for a fixed circum-circle; therefore an equilateral triangle for  $\tilde{T}$  is of optimal-shape.

If  $f(x, y)$  is not convex but has a saddle-shaped graph ( $\det(H) < 0$ ,  $\epsilon = -1$ ), then

$$\begin{aligned}
 \tilde{E}_T(\tilde{x}, \tilde{y}) &= \tilde{E}_T(\tilde{x}_c + d\tilde{x}, \tilde{y}_c + d\tilde{y}) \\
 (2.6) \qquad \qquad &= E_T - \frac{1}{2}((d\tilde{x})^2 - (d\tilde{y})^2) \\
 &= E_T - \frac{1}{2}((\tilde{x} - \tilde{x}_c)^2 - (\tilde{y} - \tilde{y}_c)^2) .
 \end{aligned}$$

We note that the error function  $\tilde{E}_T(\tilde{x}, \tilde{y})$  is a harmonic function and thus attains its extrema on the boundary of  $\tilde{T}$ . By calculus, we can show that the local extrema along edge  $(\tilde{x}_i, \tilde{y}_i)$ ,  $(\tilde{x}_j, \tilde{y}_j)$  is attained at the midpoint with value

$$\tilde{E} \left( \frac{\tilde{x}_i + \tilde{x}_j}{2}, \frac{\tilde{y}_i + \tilde{y}_j}{2} \right) = \frac{1}{8} |(\tilde{x}_i - \tilde{x}_j)^2 - (\tilde{y}_i - \tilde{y}_j)^2| .$$

The details for finding the optimal-shape triangle in this case are found in [2]. The optimal-shape triangle geometry that minimizes the efficiency ratio (Error/Area) is not unique, but the same maximum error is attained at the mid-point of each edge.

From the above two results on optimal-shape triangles, we see that a *regular* mesh of optimal-shape triangles over the isotropic  $(\tilde{x}, \tilde{y})$ -space corresponds to an optimally efficient mesh over the original  $(x, y)$ -space. Every triangle attains the same

maximum error; moreover, these triangles cover the most area for the error attained and so are optimally efficient. Since the linear transformation  $S$  is basically a rotation followed by a rescaling of coordinate axes, we find the areas of triangles are scaled accordingly. Hence the inverse transformation  $S^{-1}$ , maps this regular mesh to produce an optimally efficient mesh in the original  $(x, y)$ -space.

**2.3. Differential Geometry.** The *constant* Hessian Matrix  $H$  in (2.1) determines the coordinate transformation  $S$  that maps  $[\tilde{x}, \tilde{y}]^t = S[x, y]^t$  so that

$$[dx, dy]H[dx, dy]^t = (d\tilde{x}^2 + \epsilon d\tilde{y}^2) .$$

For more general functions, we may view the Hessian matrix  $H(x, y)$  as a metric tensor for measuring the interpolation error  $[dx, dy]H[dx, dy]^t$ . Thus we need to determine  $(\tilde{x}(x, y), \tilde{y}(x, y))$ , a *continuous* transformation that satisfies  $[dx, dy]H[dx, dy]^t = d\tilde{x}^2 + \epsilon d\tilde{y}^2$ . The conditions for finding the anisotropic coordinate transformation  $(\tilde{x}(x, y), \tilde{y}(x, y))$  are given by a classical result in differential geometry for characterizing a “flat” space [9]: that the Riemann-Christoffel tensor formed from the metric tensor  $H$  is identically zero. In this case, a sufficient condition is for  $H = \{h_{ij}\}$  to satisfy

$$K_1 h_{11} + K_2 h_{12} + K_3 h_{22} = 0$$

for some constants  $K_1, K_2, K_3$ . The coordinate transformation  $(\tilde{x}(x, y), \tilde{y}(x, y))$  may be found by solving an initial value ordinary differential equation. Again, the inverse transformation  $(x(\tilde{x}, \tilde{y}), y(\tilde{x}, \tilde{y}))$  maps a regular mesh of optimal shaped triangles to yield an optimally efficient mesh.

**3. Quadrilateral Patch.** In this section, we derive the error term for bilinear approximation of a quadratic data function.

We shall use the isoparametric formulation (commonly used in finite element analysis) by considering basis functions over the normalized  $(p, q)$ -space over the unit square,  $0 \leq p, q \leq 1$ . Basis functions are

$$(3.1) \quad \begin{aligned} \phi_1(p, q) &= (1-p)(1-q), & \phi_2(p, q) &= p(1-q), \\ \phi_3(p, q) &= pq, & \phi_4(p, q) &= (1-p)q, \end{aligned}$$

that satisfy  $\phi_i(x_j, y_j) = \delta_{ij}$ , and sum to one,  $1 = \sum_{i=1}^4 \phi_i(p, q)$ .

Mapping from  $(p, q)$  to the original  $(x, y)$ -space is by

$$(3.2) \quad \begin{aligned} x(p, q) &= x_1\phi_1(p, q) + x_2\phi_2(p, q) + x_3\phi_3(p, q) + x_4\phi_4(p, q) \\ y(p, q) &= y_1\phi_1(p, q) + y_2\phi_2(p, q) + y_3\phi_3(p, q) + y_4\phi_4(p, q) \end{aligned}$$

that maps vertex  $(0, 0)$  to  $(x_1, y_1)$ , vertex  $(1, 0)$  to  $(x_2, y_2)$ ,  $(1, 1)$  to  $(x_3, y_3)$  and  $(0, 1)$  to  $(x_4, y_4)$ . The bilinear interpolant (over  $(p, q)$ -space) is given by

$$(3.3) \quad p_b(x(p, q), y(p, q)) = \sum_{i=1}^4 f(x_i, y_i)\phi_i(p, q) .$$

**4. Optimal Shape.** In the following, we shall determine the best quadrilateral shape that minimizes the interpolation error. The error function for quadratic interpolation over a *parallelogram* can be shown by direct algebraic expansion (see Appendix A) to be

$$(4.1) \quad \begin{aligned} E_Q(p, q) &= p_b(x(p, q), y(p, q)) - f(x(p, q), y(p, q)) \\ &= E_Q - \frac{1}{2} (\mu_1(p - p_c)^2 + \mu_2(q - q_c)^2) , \end{aligned}$$

with centroid at  $[p_c, q_c] = [1/2, 1/2]$ ,

$$[u_x, u_y] = [x_2 - x_1, y_2 - y_1], \quad [v_x, v_y] = [x_4 - x_1, y_4 - y_1],$$

$$(4.2) \quad \begin{aligned} E_Q &= E_Q(p_c, q_c) = \frac{1}{8}(\mu_1 + \mu_2), \\ 0 &= \frac{\partial}{\partial p} E_Q(p_c, q_c) = \frac{\partial}{\partial q} E_Q(p_c, q_c), \\ \mu_1 &= [u_x, u_y]H[u_x, u_y]^t, \quad \mu_2 = [v_x, v_y]H[v_x, v_y]^t. \end{aligned}$$

For a convex function ( $\det(H) > 0$ ),  $\mu_1$  and  $\mu_2$  are positive, hence the maximum error is attained at the centroid  $[p_c, q_c]$ .

For this convex case, we can show a square over the isotropic space is of optimal shape by minimizing the efficiency ratio (Error/Area). Since the isoparametric bilinear interpolant (3.3) exactly fits linear functions [5], the error attained at the centroid  $(x_c, y_c)$  (which is a lower bound on the maximum error) can be written as

$$(4.3) \quad \begin{aligned} E_M &= \frac{1}{4} \left( \sum_{i=1}^{i=4} \frac{1}{2} [x_i, y_i] H [x_i, y_i]^t \right) - \frac{1}{2} [x_c, y_c] H [x_c, y_c]^t \\ &= \frac{1}{8} \left( \sum_{i=1}^{i=4} ([x_i, y_i] H [x_i, y_i]^t - [x_c, y_c] H [x_c, y_c]^t) \right) \end{aligned}$$

$$(4.4) \quad [x_c, y_c] = [(x_1 + x_2 + x_3 + x_4)/4, (y_1 + y_2 + y_3 + y_4)/4].$$

This expression can be further simplified over the isotropic space where  $H$  is the identity,

$$\begin{aligned} E_M &= \frac{1}{8} \left( \sum_{i=1}^{i=4} ((\tilde{x}_i^2 + \tilde{y}_i^2) - (\tilde{x}_c^2 + \tilde{y}_c^2)) \right) \\ &= \frac{1}{8} ((\tilde{x}_1^2 + \tilde{x}_2^2 + \tilde{x}_3^2 + \tilde{x}_4^2) - 4\tilde{x}_c^2 + (\tilde{y}_1^2 + \tilde{y}_2^2 + \tilde{y}_3^2 + \tilde{y}_4^2) - 4\tilde{y}_c^2) \\ &= \frac{1}{8} (L_1^2 + L_2^2 + L_3^2 + L_4^2), \quad \text{with } L_i^2 = (\tilde{x}_i - \tilde{x}_c)^2 + (\tilde{y}_i - \tilde{y}_c)^2, \end{aligned}$$

where  $[\tilde{x}_i, \tilde{y}_i]^t = S[x_i, y_i]^t$  and  $[\tilde{x}_c, \tilde{y}_c]^t = S[x_c, y_c]^t$  are the corresponding coordinates over the isotropic space. The area of this transformed convex quadrilateral is (see Figure 4.1)

$$\text{Area} = \frac{1}{2} (L_1 L_2 \sin(\theta_1) + L_2 L_3 \sin(\theta_2) + L_3 L_4 \sin(\theta_3) - L_4 L_1 \sin(\theta_1 + \theta_2 + \theta_3)).$$

Since the isotropic transformation  $S$  in (2.3) is a rotation followed by a rescaling of coordinate axis, the area of quadrilateral over the isotropic space is scaled by  $\sqrt{|\lambda_1 \lambda_2|} = \sqrt{|\det(H)|}$  (intrinsic to  $H$ ). By Calculus, we can show this ratio of  $E_M/\text{Area}$  is minimized and *attained* by a square with  $L_1 = L_2 = L_3 = L_4$  and  $\theta_1 = \theta_2 = \theta_3 = \pi/4$ . Hence the most efficient shape among *all* general convex bilinear quadrilaterals is a square over the isotropic space with an efficiency ratio of  $1/4$ .

If  $f(x, y)$  is saddle-shaped ( $\det(H) < 0$ ), the error expression for a parallelogram is still

$$E_Q(p, q) = \frac{1}{8}(\mu_1 + \mu_2) - \frac{1}{2}(\mu_1(p - p_c)^2 + \mu_2(q - q_c)^2).$$

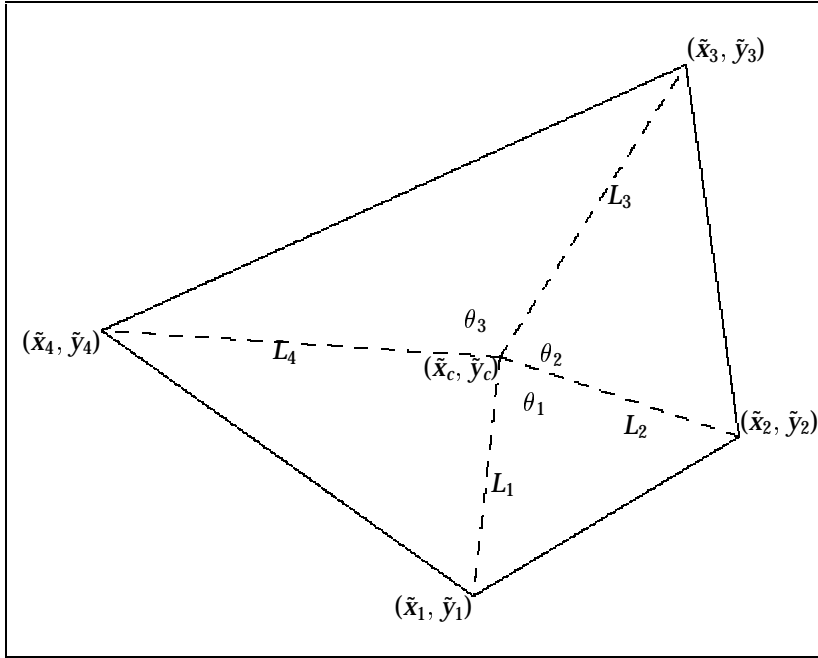


FIG. 4.1. Convex quadrilateral over isotropic space.

Under the anisotropic transformation  $S$ ,

$$\mu_1 = \tilde{u}_x^2 - \tilde{u}_y^2, \quad \mu_2 = \tilde{v}_x^2 - \tilde{v}_y^2, \quad \begin{bmatrix} \tilde{u}_x & \tilde{v}_x \\ \tilde{u}_y & \tilde{v}_y \end{bmatrix} = S \begin{bmatrix} u_x & v_x \\ u_y & v_y \end{bmatrix}.$$

Now both  $\mu_1$  and  $\mu_2$  vanish for

$$(4.5) \quad [\tilde{u}_x, \tilde{u}_y] = [L, L], \quad [\tilde{v}_x, \tilde{v}_y] = [-L, L],$$

which correspond to a square rotated by  $\pi/4$ . The above indicates an “exact fit” ( $E_Q(p, q) = 0$ ) if  $\mu_1 = \mu_2 = 0$ . This suggests bilinear approximation is a better interpolant than linear interpolation and the simple quadratic model is inadequate to fully capture the error properties in this case.

To summarize, a square over the isotropic space in any orientation is optimal for the elliptic case, and a square rotated by  $\pi/4$  is optimal for the hyperbolic case.

**5. Comparison of quadrilaterals versus triangles.** In this section, we shall show a refined triangulation produced by the Delauney Triangulation (DT) will always produce better accuracy for approximating a convex quadratic function. We shall apply the geometric interpretation of the maximum interpolation error over the transformed isotropic space.

**THEOREM 5.1.** *Any convex quadrilateral over the isotropic space can be decomposed into two triangles with no increase in maximum interpolation error for approximating a convex quadratic.*

*Proof.* We shall use the Delauney Triangulation (DT) [3] in selecting the diagonal for decomposing the general convex quadrilateral into two triangles. The DT has an interesting properties that three vertices form a triangle in DT iff no other vertex is

interior to the circum-circle formed by these vertices. This is also commonly known as the “empty circle” property.

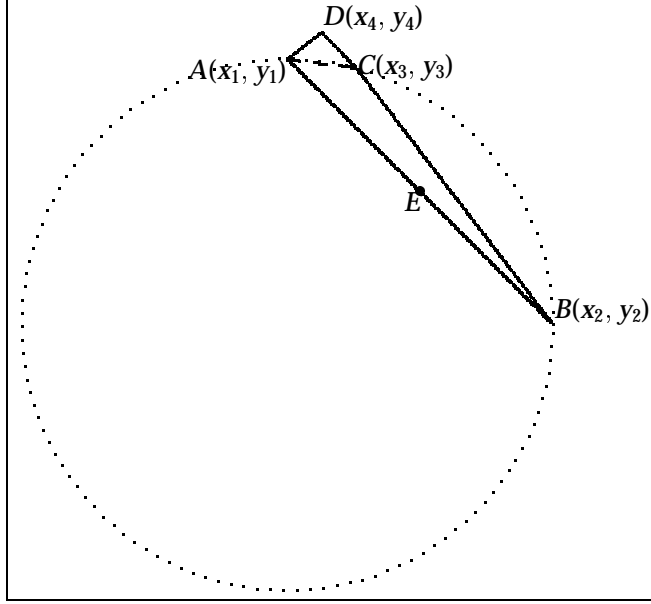


FIG. 5.1. Maximum triangulation error attained on boundary edge.

*Case 1.* The maximum error of the DT is attained at the mid-point ( $E$ ) of a boundary edge (see Figure 5.1). In this case the error attained is due to linear interpolation along the edge  $AB$ , with value  $|AB|^2/8$ . Since the isoparametric bilinear interpolant over the quadrilateral also reduces to linear interpolation along the boundary edge, the maximum error for bilinear quadrilateral cannot be less than this value. Therefore the theorem holds.

*Case 2.* The maximum error of the DT is attained at the center of circum-circle,  $(x_c, y_c)$  (see Figure 5.2). For simplicity and without loss of generality, we perform a translation such that the isotropic quadratic data function is  $\frac{1}{2}((x - x_c)^2 + (y - y_c)^2)$ . The maximum error is  $R^2/2$ , where  $R$  is the radius of the circum-circle. The interpolation error given by the quadrilateral is (3.3),

$$(5.1) \quad \begin{aligned} E_Q(x_c, y_c) &= \left( \sum_{i=1}^{i=4} f_i \phi_i(p, q) \right) - f(x_c, y_c), \quad f_i = f(x_i, y_i) \\ &= ((1 - \phi_3(p, q))R^2/2 + \phi_3(p, q) f_3) - 0 \end{aligned}$$

since  $f_1 = f_2 = f_3 = R^2/2$  and  $f(x_c, y_c) = 0$ . We have

$$(5.2) \quad f(x_3, y_3) = ((x_3 - x_c)^2 + (y_3 - y_c)^2)/2 > R^2/2,$$

and therefore the error attained by quadrilateral at  $(x_c, y_c)$  is higher than  $R^2/2$ , thus the theorem holds.

Cases 1 and 2 are exhaustive since the maximum error of the DT cannot be attained at the the mid point of a diagonal, unless it also satisfies Case 1 or Case 2 as in a square (see Figure 5.3). We have  $\angle BCD \leq \pi/2$  to satisfy the “empty circle”

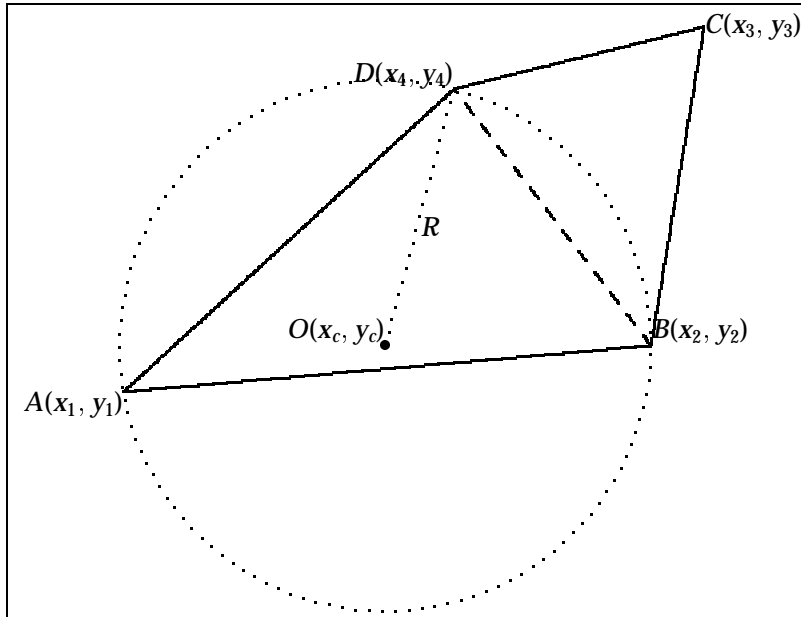


FIG. 5.2. Maximum triangulation error attained at center of circum-circle.

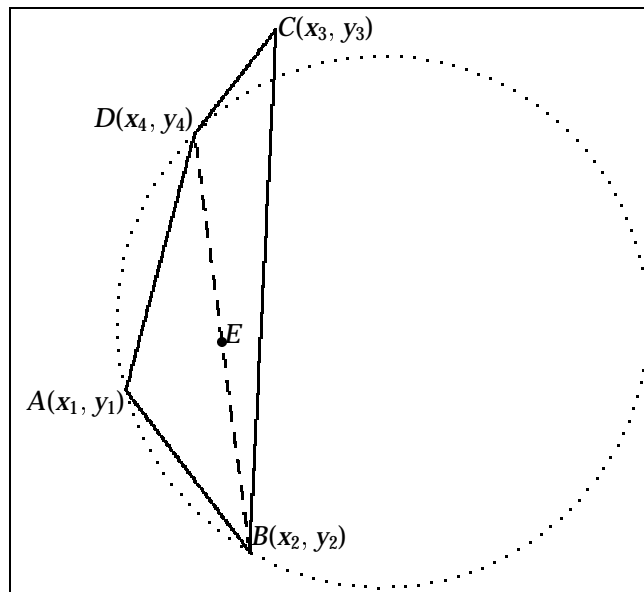


FIG. 5.3. Maximum triangulation error cannot be on diagonal.

property. If  $\angle CDB > \pi/2$  (similar argument for  $\angle CBD > \pi/2$ ), then by Cosine rule for triangles,

$$(5.3) \quad |BC|^2 = |CD|^2 + |BD|^2 - 2|CD||BD|\cos(\angle CDB) > |BD|^2,$$

thus the maximum error is attained in  $\triangle BCD$  on edge  $BC$  (Case 1). The remaining alternative is where  $\triangle BCD$  forms an acute triangle. Then  $\triangle BCD$  will have a larger

maximum error given in terms of radius of circum-circle, which is covered in Case 2.

Therefore over the isotropic space, the DT refined linear triangulation is more accurate than the isoparametric bilinear quadrilateral.  $\square$

This theorem suggests if the data function is not saddle-shaped, the refine DT triangulation (over the isotropic space) produced above will yield better approximation accuracy, even on arbitrary meshes of general convex quadrilaterals.

**5.1. Comparison of efficiency ratio.** For the optimal shape equilateral triangle, the area,  $A_T$ , is  $\sqrt{3}L^2/4$ , from (2.4) we obtain an efficiency ratio of

$$\frac{E_T}{A_T} = \frac{L^2/6}{\sqrt{3}L^2/4} = 2\sqrt{3}/9 \approx 0.385 .$$

Area of the optimal square configuration is  $L^2$ , thus the ratio is  $1/4 = 0.25$ . Hence for an *element by element* comparison, the quadrilateral is more efficient. In other words, if we were to approximate a function with either  $N$  quadrilaterals or  $N$  triangles, quadrilaterals are preferred.

On the other hand, triangles may have advantages over quadrilaterals for finite element computations. Matrix assembly and the solution of the sparse linear equations are commonly the most intensive calculations. If we decompose a quadrilateral mesh into triangles as done above, no extra nodes are introduced. There will be twice as many triangular elements but the resulting assembled matrix has a similar sparsity pattern and the same number of unknowns. Matrix assembly with a *general* convex quadrilateral usually requires costly evaluations of the Jacobian distortion in numerical quadrature over the isoparametric space, whereas assembly of linear triangle elements is simpler. Therefore if computation with  $N$  quadrilaterals is as costly as using  $2N$  triangles, then triangles are preferred due to their better accuracy and simplicity. The actual computation costs may depend on the implementation of the finite element code.

Consider the approximation of a saddle-shaped function by a square (unrotated) over the isotropic space. The error formula gives

$$(5.4) \quad \begin{aligned} E_Q(p, q) &= \frac{1}{8}(\mu_1 + \mu_2) - \frac{1}{2}(\mu_1(p - p_c)^2 + \mu_2(q - q_c)^2), \quad (p_c, q_c) = (\frac{1}{2}, \frac{1}{2}) \\ &= -\frac{1}{2}((p - p_c)^2 L^2 - (q - q_c)^2 L^2), \quad \text{where } \mu_1 = L^2 = -\mu_2 . \end{aligned}$$

The maximum error is attained at the mid-point of each edge. Let  $(p, q) = (1, 1/2)$ , then  $E_Q = L^2/8$ . This gives an efficiency ratio of  $1/8 = 0.125$ . One optimal triangle shape for saddle-shaped function is the triangle with vertices at  $(0, 0)$ ,  $(L, 0)$ ,  $(1/2L, \sqrt{5}/2L)$  over the isotropic space [2], which has area  $\sqrt{5}L^2/4$ . The maximum error is  $L^2/8$  and attained at the mid-point of each edge. This gives an efficiency ratio of  $1/(2\sqrt{5}) \approx 0.224$ . Thus over the isotropic space, a mesh with  $N$  (unrotated) squares should yield roughly the same accuracy as  $2N$  triangles. This is verified in the numerical experiments.

**6. Numerical Experiments.** In this section, we demonstrate that a well designed mesh for bilinear interpolation of a saddle-shaped function may give substantial improvements over a triangular mesh. The examples are taken from [2]. The procedure in [2] for generating optimal triangular meshes is modified to generate optimal quadrilateral meshes. Only elements entirely interior to the unit square are generated to simplify the presentation.

*Example 1.* Exponential increase along  $x$ -axis,

$$f(x, y) = \exp(5x) \sin(5y) .$$

*Example 2.* A near singularity at  $(x_0, y_0) = (0.5, -0.2)$ ,

$$f(x, y) = \frac{(x - x_0)^2 - (y - y_0)^2}{((x - x_0)^2 + (y - y_0)^2)^2} .$$

*Example 3.* A more severe near singularity,

$$f(x, y) = \frac{((x - x_0)^2 + (y - y_0)^2)^2 - 8(x - x_0)^2(y - y_0)^2}{((x - x_0)^2 + (y - y_0)^2)^4} .$$

*Example 4.* Example 4 is Example 2 modified by a rescaling of  $y$ -axis,

$$f(x, y) = \frac{(x - x_0)^2 - (\sqrt{10}y - y_0)^2}{((x - x_0)^2 + (\sqrt{10}y - y_0)^2)^2} .$$

The results of the experiments are summarized in Figures 6.1–6.4 and Tables 6.1–6.4. Mesh I is generated by optimal squares over the isotropic space. Mesh II is generated by optimal squares with a  $\pi/4$  rotation over the isotropic space to capture the “super-convergence” behavior. Both meshes have similar element size, element shape and density and differ mainly in their orientation. The meshes are displayed in Figures 6.5–6.12. Results for optimal triangular meshes produced in [2] are included for comparison. Mesh I produces an almost level error profile. This indicates an equilibration of interpolation error evenly over all elements. Error profile for Mesh I is roughly comparable to an optimal triangular mesh with about twice as many triangles and in agreement with discussions in §5. Mesh II displays the “super-convergence” behavior by consistently achieving an error 5–10 times smaller than Mesh I.

Table 6.5 shows the effect of generating finer meshes over the isotropic space. If we consider the median error, Mesh I shows the expected  $O(h^2)$  convergence. From the efficiency ratio (Error/Area), we can also predict the decrease of error is proportional to the number of elements. Results for Mesh II clearly display the higher than  $O(h^2)$  “super-convergence” behavior. From another perspective, about 5–10 times *more* elements are needed for Mesh I to match the accuracy of Mesh II.

It can be shown [1] that the coordinate lines in the isotropic space are mapped to eigen-trajectories of the Hessian matrix. Thus as the curved element boundaries are poorly approximated by straight edges, the resulting quadrilateral will no longer have parallel sides (Fig. 6.9, 6.10). The simple analysis for super-convergence in §3 for parallelograms may not be adequate and this leads to an anomalous increase in the error displayed in Example 3 of a severe singularity.

**7. Summary.** We have used a simple locally quadratic model to develop a geometric interpretation of the interpolation error. We determine the optimal element shapes and their efficiency ratio (Error/Area) over the isotropic space. The analysis shows for approximating convex data functions, although bilinear quadrilaterals are more efficient, linear triangles are more accurate and may be preferred in finite element computations. For approximating saddle-shaped data functions, a well designed quadrilateral mesh may show “super-convergence” improvements in approximation accuracy. Numerical experiments show good agreement with the analysis, and a surprising finding is different grid orientations may have an order of magnitude improvement in accuracy.

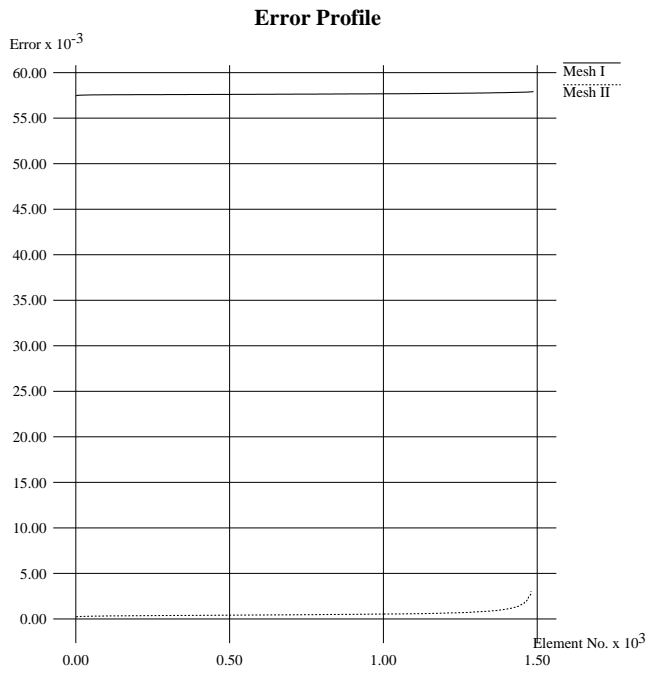


FIG. 6.1. Error profiles for Example 1.

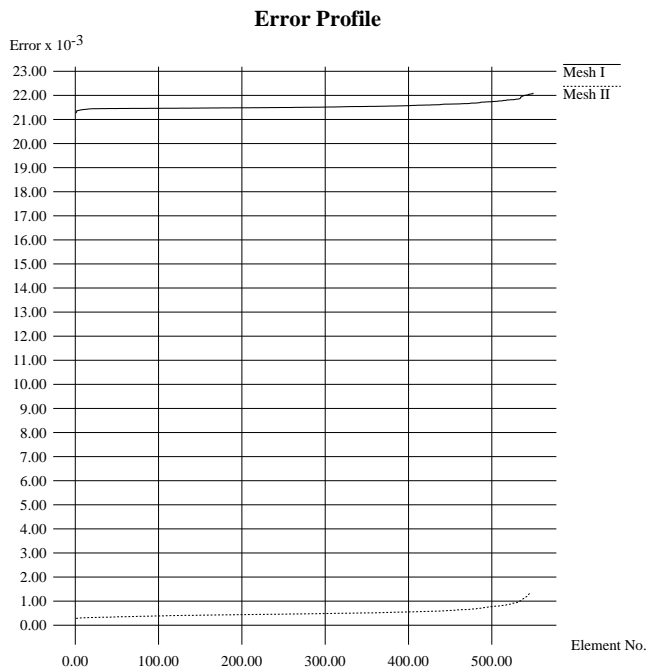


FIG. 6.2. Error profiles for Example 2.

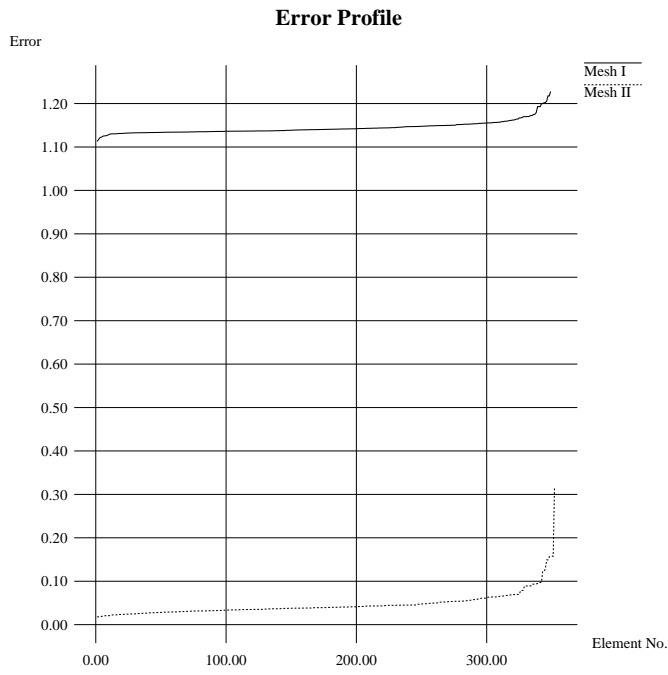


FIG. 6.3. Error profiles for Example 2.

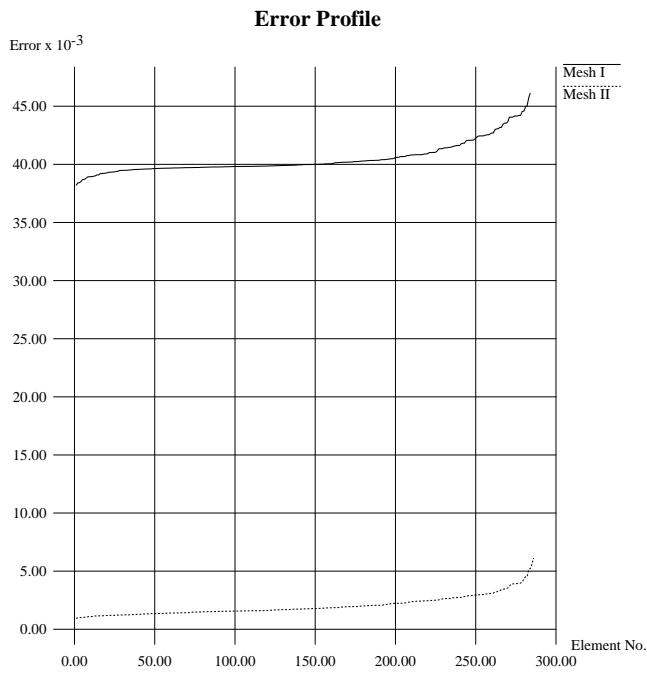


FIG. 6.4. Error profiles for Example 3.

TABLE 6.1  
Summary of results for Example 1.

	Minimum error	Median error	90 percentile	Maximum error	Number of elements
Triangle	5.27E-2	5.39E-2	5.50E-2	5.74E-2	2923
Mesh I	5.75E-2	5.76E-2	5.78E-2	5.79E-2	1488
Mesh II	2.29E-4	4.62E-4	8.30E-4	3.04E-3	1480

TABLE 6.2  
Summary of results for Example 2.

	Minimum error	Median error	90 percentile	Maximum error	Number of elements
Triangle	1.87E-2	2.01E-2	2.16E-2	2.57E-2	1072
Mesh I	2.13E-2	2.15E-2	2.17E-2	2.21E-2	550
Mesh II	2.82E-4	4.69E-4	7.33E-4	1.38E-3	546

TABLE 6.3  
Summary of results for Example 3.

	Minimum error	Median error	90 percentile	Maximum error	Number of elements
Triangle	1.02	1.16	1.32	1.70	650
Mesh I	1.11	1.14	1.16	1.23	349
Mesh II	1.80E-2	3.94E-2	6.75E-2	3.16E-1	352

TABLE 6.4  
Summary of results for Example 4.

	Minimum error	Median error	90 percentile	Maximum error	Number of elements
Triangle	2.91E-2	3.68E-2	4.61E-2	6.46E-2	608
Mesh I	3.81E-2	4.00E-2	4.24E-2	4.61E-2	284
Mesh II	9.36E-4	1.76E-3	3.04E-3	6.13E-3	286

TABLE 6.5  
Convergence test on Example 3.

	Minimum error	Median error	90 percentile	Maximum error	Number of elements
Mesh I	11.1E-1	11.4E-1	11.6E-1	12.3E-1	349
Mesh I	3.22E-1	3.23E-1	3.24E-1	3.26E-1	1223
Mesh I	8.03E-2	8.07E-2	8.12E-2	8.23E-2	5063
Mesh I	1.99E-2	2.02E-2	2.04E-2	2.08E-2	20603
Mesh II	1.80E-2	3.94E-2	6.75E-2	3.16E-1	352
Mesh II	2.35E-3	4.22E-3	9.16E-3	6.35E-2	1260
Mesh II	3.10E-4	7.20E-4	1.29E-3	9.41E-3	5244
Mesh II	5.19E-5	1.79E-4	3.78E-4	1.24E-3	21389

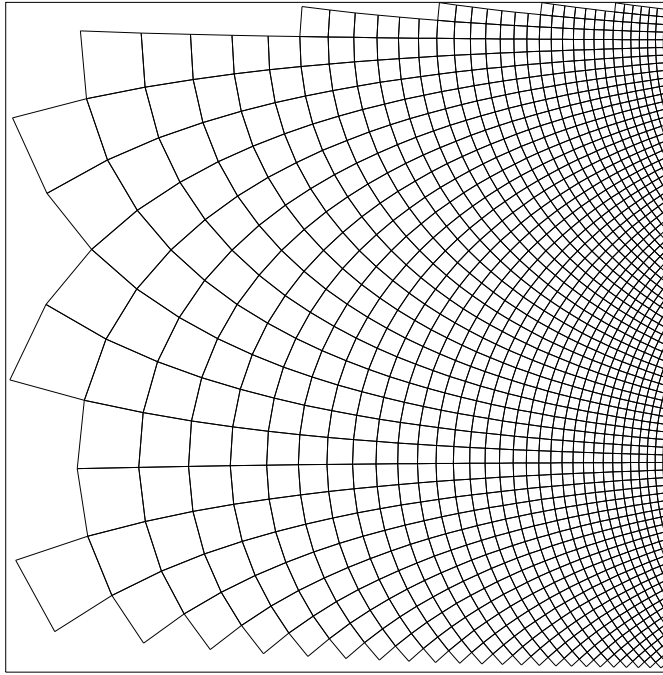


FIG. 6.5. Mesh I for Example 1.

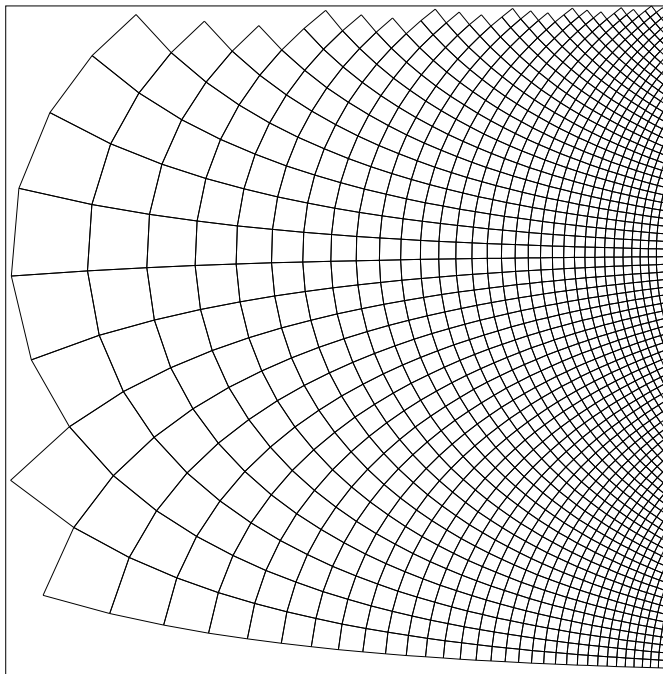


FIG. 6.6. Mesh II for Example 1.

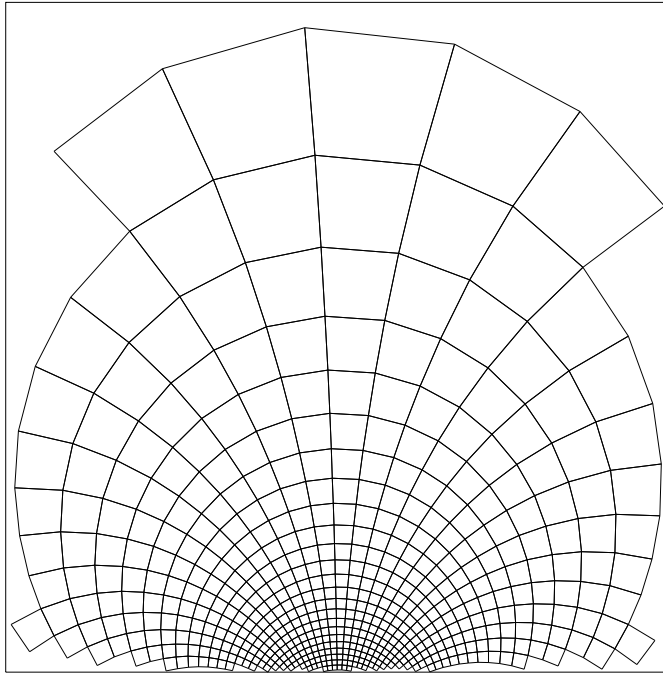


FIG. 6.7. Mesh I for Example 2.

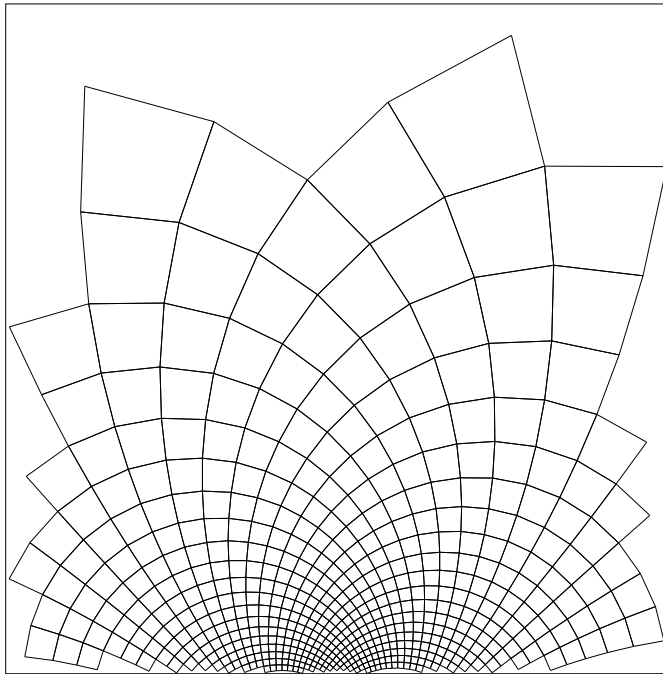


FIG. 6.8. Mesh II for Example 2.

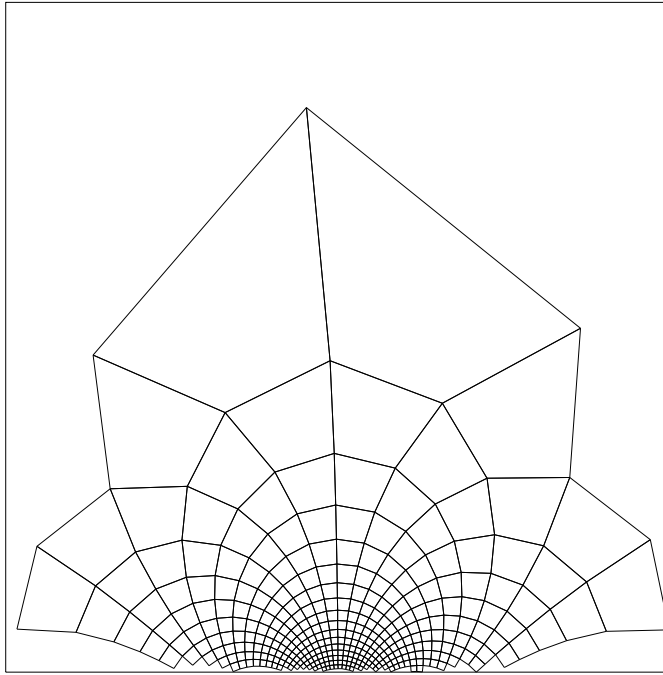


FIG. 6.9. Mesh I for Example 3.

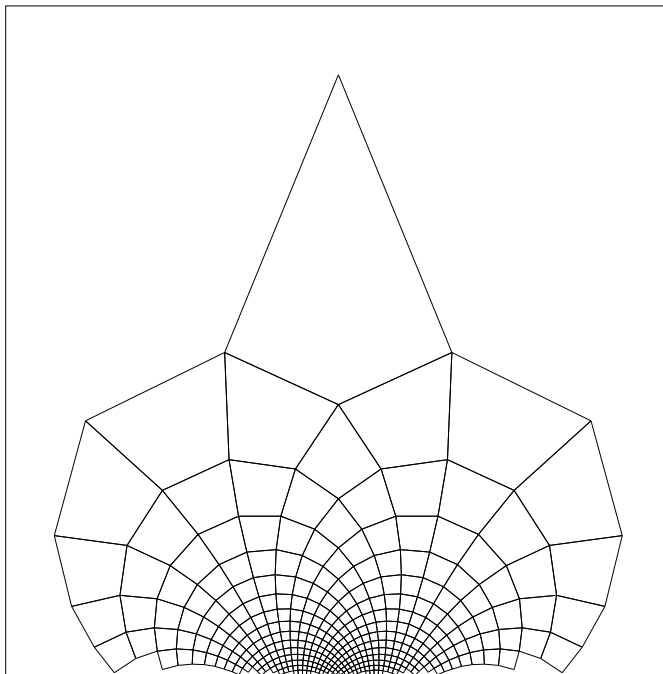


FIG. 6.10. Mesh II for Example 3.

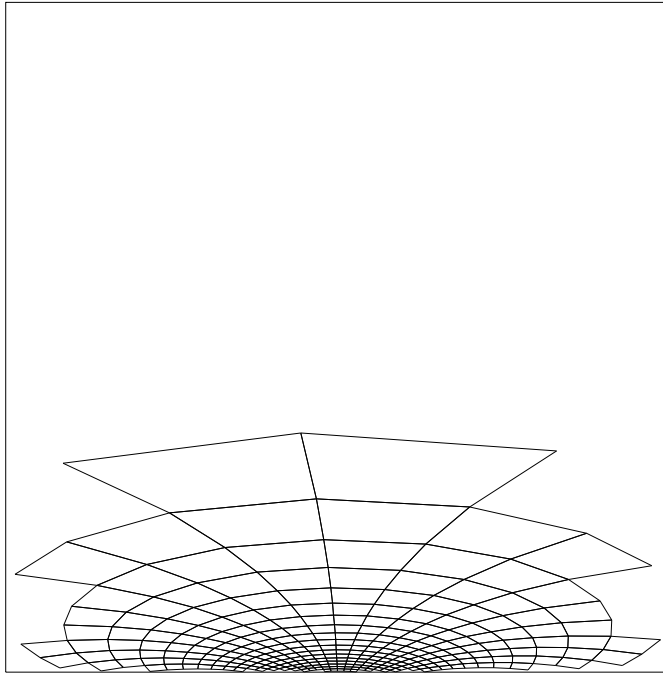


FIG. 6.11. Mesh I for Example 4.

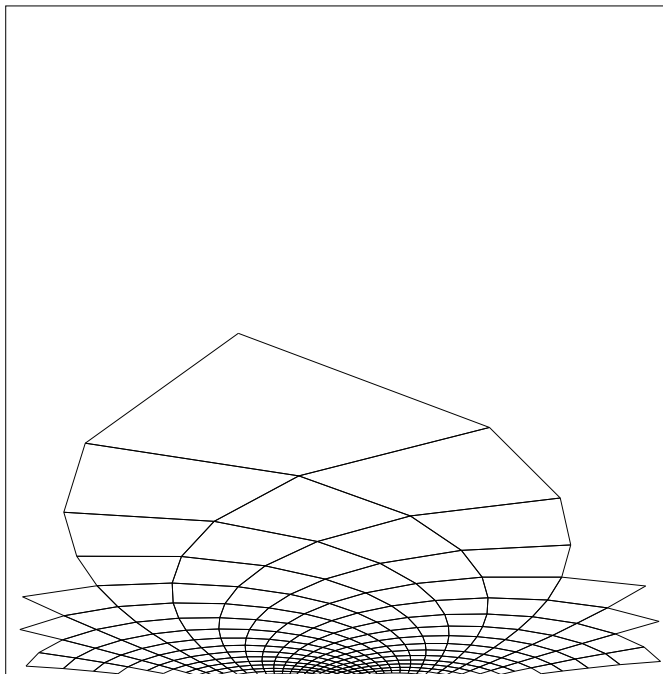


FIG. 6.12. Mesh II for Example 4.

**Appendix A.** In this section, we show the error function for quadratic interpolation over a parallelogram is given by (4.1) by simple algebraic expansion. Let the data function be

$$(7.1) \quad f(x, y) = \frac{1}{2}[x, y]H[x, y]^t + [g_1, g_2][x, y]^t + c$$

and the affine isoparametric transformation be

$$(7.2) \quad \begin{bmatrix} x(p, q) \\ y(p, q) \end{bmatrix} = T \begin{bmatrix} p \\ q \end{bmatrix} + \begin{bmatrix} x_1 \\ y_1 \end{bmatrix}, \quad T = \begin{bmatrix} u_x & v_x \\ u_y & v_y \end{bmatrix} = \begin{bmatrix} x_2 - x_1 & x_4 - x_1 \\ y_2 - y_1 & y_4 - y_1 \end{bmatrix}.$$

Then the interpolation error can be shown to be

$$(7.3) \quad \begin{aligned} E_Q(p, q) &= p_t(x(p, q), y(p, q)) - f(x(p, q), y(p, q)) \\ &= E_Q - \frac{1}{2}(\mu_1(p - p_c)^2 + \mu_2(q - q_c)^2), \end{aligned}$$

with centroid at  $[p_c, q_c] = [\frac{1}{2}, \frac{1}{2}]$ ,

$$\begin{aligned} E_Q &= E_Q(p_c, q_c) = \frac{1}{8}(\mu_1 + \mu_2), \\ \mu_1 &= [u_x, u_y]H[u_x, u_y]^t, \quad \mu_2 = [v_x, v_y]H[v_x, v_y]^t \end{aligned}$$

Let the data function over  $(p, q)$ -space be written as

$$(7.4) \quad \begin{aligned} \tilde{f}(p, q) &= f(x(p, q), y(p, q)) \\ &= \frac{1}{2}[p, q]\tilde{H}[p, q]^t + [\tilde{g}_1, \tilde{g}_2][p, q]^t + \tilde{c} \end{aligned}$$

where  $\tilde{H} = T^t H T = \begin{bmatrix} \tilde{h}_{11} & \tilde{h}_{12} \\ \tilde{h}_{12} & \tilde{h}_{22} \end{bmatrix}$  and

$$(7.5) \quad \begin{aligned} [\tilde{g}_1, \tilde{g}_2] &= ([g_1, g_2] + [x_1, y_1]H) T, \\ \tilde{c} &= c + [g_1, g_2][x_1, y_1]^t + \frac{1}{2}[x_1, y_1]H[x_1, y_1]^t. \end{aligned}$$

The function values at the four interpolating corners are

$$(7.6) \quad \begin{aligned} f_1 &= \tilde{f}(0, 0) = \tilde{c}, \quad f_3 = \tilde{f}(1, 1) = \frac{1}{2}(\tilde{h}_{11} + \tilde{h}_{22} + 2\tilde{h}_{12}) + \tilde{g}_1 + \tilde{g}_2 + \tilde{c}, \\ f_2 &= \tilde{f}(1, 0) = \frac{1}{2}\tilde{h}_{11} + \tilde{g}_1 + \tilde{c}, \quad f_4 = \tilde{f}(0, 1) = \frac{1}{2}\tilde{h}_{22} + \tilde{g}_2 + \tilde{c}. \end{aligned}$$

By (3.3) and (7.3) (note the vanishing of linear and constant terms),

$$\begin{aligned} E_Q(p, q) &= \left( \sum_{i=1}^{i=4} f_i \phi_i(p, q) \right) - \tilde{f}(p, q) \\ &= \frac{1}{2} (p(1 - q)\tilde{h}_{11} + pq(\tilde{h}_{11} + \tilde{h}_{22} + 2\tilde{h}_{12}) \\ &\quad + (1 - p)q\tilde{h}_{22} - (p^2\tilde{h}_{11} + q^2\tilde{h}_{22} + 2pq\tilde{h}_{12})) \end{aligned}$$

$$\begin{aligned}
&= \frac{1}{2} (p\tilde{h}_{11} + q\tilde{h}_{22} + 2pq\tilde{h}_{12} - p^2\tilde{h}_{11} - q^2\tilde{h}_{22} - 2pq\tilde{h}_{12}) \\
&= \frac{1}{2} (p(1-p)\tilde{h}_{11} + q(1-q)\tilde{h}_{22}) \\
(7.7) \quad &= \frac{1}{8} (\tilde{h}_{11} + \tilde{h}_{22}) - \frac{1}{2} (\tilde{h}_{11}(p - \frac{1}{2})^2 + \tilde{h}_{22}(q - \frac{1}{2})^2).
\end{aligned}$$

From (7.2) and (7.4), we have  $\tilde{h}_{11} = \mu_1$  and  $\tilde{h}_{22} = \mu_2$ ; hence the error function has the form given in (7.3).

## REFERENCES

- [1] E. F. D'AZEVEDO, *On Optimal Triangulation for Piecewise Linear Approximation* PhD thesis, Department of Computer Science, University of Waterloo, Waterloo, Ontario, Canada, 1989.
- [2] ———, *Optimal triangular mesh generation by coordinate transformation* SIAM J. Sci. Statist. Comput., 12 (1991), pp. 755–786.
- [3] E. F. D'AZEVEDO AND R. B. SIMPSON, *On optimal interpolation incidences* SIAM J. Sci. Statist. Comput., 10 (1989), pp. 1063–1075.
- [4] ———, *On optimal triangular meshes for minimizing the gradient error*, Numer. Math., 59 (1991), pp. 321–348.
- [5] A. R. MITCHELL AND R. WAIT, *The Finite Element Methods in Partial Differential Equations* Wiley-Interscience Publication, 1977.
- [6] E. NADLER, *Piecewise linear best  $l_2$  approximation on triangulations* in Approximation Theory V, C. K. Chui, L. L. Schumaker, and J. D. Ward, eds., Boston, 1986, Academic Press, pp. 499–502.
- [7] J. PERAIRE, M. VAHDATI, K. MORGAN, AND O. C. ZIENKIEWICS, *Adaptive remeshing for compressible flow computations*, J. Comput. Phys., 72 (1987), pp. 449–466.
- [8] R. B. SIMPSON, *Anisotropic mesh transformations and optimal error control* Applied Numerical Mathematics, (1992). Special issue as the proceedings of the US Army sponsored Workshop for Adaptive Methods for Partial Differential Equations, Rensselaer Polytechnical Institute (accepted).
- [9] I. S. SOKOLNIKOFF, *Tensor Analysis, Theory and Applications to Geometry and Mechanics of Continua* John Wiley, New York, second ed., 1964.